Simulating the Interactions Among Vasomotion Waves of Peripheral Vascular Districts

G Baselli, A Porta

Dept. of Bioengineering, Polytechnic University of Milan, Italy
Dept. of Preclinical Sciences, LITA Vialba, University of Milan, Italy

Abstract

Simulations are performed in order to analyze the tendency of oscillating peripheral vascular districts (PVDs) to maintain equal phases thus inducing low frequency (LF) waves in systemic arterial pressure (AP).

A PVD model regulating the local flow by means of a delayed non-linear feedback displayed spontaneous oscillations with a 12 sec period in the pressure range (40 - 150 mmHg) of active flow compensation.

Two identical PVDs loading the same windkessel compartment could oscillate in phase inducing significant (10% of mean) AP waves; however, this behavior was unstable. On the contrary, phase opposition (without AP waves) was stable and corresponded to an energetic minimum (-9 % compared to the unstable solution).

The introduction of either baroreflex mechanisms or a central drive was able to steadily align the PVD phases. Vasomotion synchronization can be a powerful modulation mechanism of LF waves in systemic AP.

1. Introduction

The low frequency (LF) oscillations displayed by cardiovascular variability have been intensively studied as a marker of autonomic regulation mainly related to sympathetic activation [1]. Besides the eventual participation of central drives, the main contribution of vasomotion and vascular control mechanisms is generally recognized as origin of LF AP waves (Mayer's waves) [2], hence reflected on other signals such as heart rate variability.

In this perspective, the importance of inner instabilities of baroreflex regulation of systemic AP is often stressed in the models trying to explain and reproduce Mayer's waves [3,4]. Indeed, evidences have been brought about relevant to the scarce capability of AP control in damping oscillations in the LF range, due to the inherent delays in the effector mechanisms, mainly the modulation of total peripheral resistances (TPR).

This approach, however, may miss the obvious physiological concept that AP control is secondary to the regulation of flows feeding the single peripheral districts.

In other words, TPR is a mere abstraction of the total effect of parallel peripheral districts, which are lumped together from the point of view of systemic AP. Even more importantly, it is not recognized the active contribution given by vasomotion in small peripheral arteries to the perfusion of tissues.

Vasomotion in microvessels is intensively studied and various models relevant to its periodic, quasi-periodic, intermittent and chaotic activity have been proposed [5,6]. Mechanisms taken into account for the dynamic changes in arteriolar diameter include: myogenic response, endothelial shear stress, oscillations in Ca^{++} transmembrane exchange, and in intracellular Ca^{++} storage [2,5,6].

The present approach does not focus directly the local mechanisms inducing vasomotion; it simply hypothesizes a generic (or lumped) mechanism of local flow control elicited with the delays inherent to the response of smooth muscles. Consequently, considerations are drawn relevant to the hemodynamic coupling of peripheral districts by loading common windkessel compartments. The main question addressed is whether hemodynamic effects *per se*, in the absence of neural modulation, are able to induce synchronization of different districts or not and (if not) to what degree the synchronization necessary to induce AP waves at systemic level can be paced by neural outflows: either central, or sympathetic, or baroreflex related [7,8].

2. Simple arterial tree model

Fig.1 displays an extremely simplified and idealized arterial tree in which the cardiac output feeds a several branching windkessel compartments. As it can be noticed, an indiscriminate binary tree is considered; nonetheless, a more realistic description of the subdivision of flows directed to the head, splancnic districts, upper and lower limbs, etc. could be easily imposed by a proper definition of arterial and peripheral district parameters.

Windkessel compartments are present at each branching level and are hypothesized to include large compliances and small resistances in the first branches (aorta and the largest arteries) and, on the contrary, to be

0276−6547/02 $17.00 © 2002 IEEE

Computers in Cardiology 2002;29:49−52.

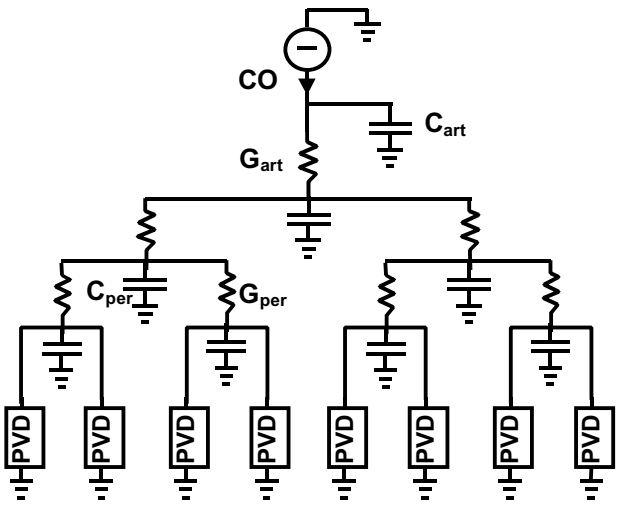

Fig.1 - Simple arterial tree model.

stiffer and more resistant towards the periphery. Nonetheless, the total compliance of peripheral levels can be sensible due to the high number of branches that are added. Compliance and conductance (preferred to resistance, as summable in parallel branches) parameters are adjusted in order to obtain the desired time constant of the lumped windkessel relevant to the whole tree: $T_{lumped} = C_{lumped} / G_{lumped}$; where C_{lumped} is the total compliance of the tree and similarly G_{lumped} is the inverse of the TPR seen from the aorta. T_{lumped} = 2 sec is generally assumed and its value is tested in pulsatile regime. The distribution of compliances and conductances at the various branching levels is adjusted in order to obtain the desired fall in AP from center to periphery and a reliable decrease of pulse pressure in pulsatile regime.

The final branches of the tree are represented by peripheral vascular districts (PVDs) which actively control their own input flows in the proximity of their working points represented by a nominal flow, F_0, and nominal driving pressure, P_0. Their nominal conductance $G_0 = F_0/P_0$ must be taken into account in the above described settings of the arterial tree parameters. In addition, the sum of all nominal conductances should be matched to the imposed feeding flow (cardiac output, CO, if the whole body is considered) for an isovolemic condition. As to the dimension of single PVDs (represented by their nominal flow) it can span from arteriolar districts up to organ or limb level; obviously an atomization into many small districts implies less a priori constraints, while grouping some districts into a larger one implies an assumption of synchronized activity among them.

3. Single PVD characteristics

The Simulink® (graphic interface of Matlab®) block diagram of the PVD model is shown in Fig.2. The conductance profile g(P) is a threshold/saturation function of driving pressure P(t): below 20 mmHg the vessel is considered collapsed and g(P)=0, above 40 mmHg the nominal conductance G_0 is reached, a linear increase is described in-between. The conductance is further modulated both by a local feedback based on flow deficit and by neural activity. The former effect is a third power-law of the ratio between the nominal flow and the actual flow, $(F_0/F(t))^3$; thus it equals 1 (no modulation) when $F(t)=F_0$, it strongly enhances conductance when there is a lack of flow, while a weaker opposite effect is elicited with flow excess. The neural modulation is 1 in the denervated or basal activity levels, while an inverse power low with the firing of sympathetic fibers can be considered to describe the subsequent vasoconstriction. The modulating action is supposed to saturate below a factor of 1/2 and above 2 and it is elicited through a time delay of 4 sec and a time constant of 3 sec accounting for the sluggish activation of smooth muscles and also of the slow metabolic response to flow imbalance.

A single PVD driven by an increasing pressure displays the following features: 1) vessels are collapsed below 20 mmHg; 2) in a wide range (40 to 150 mmHg)

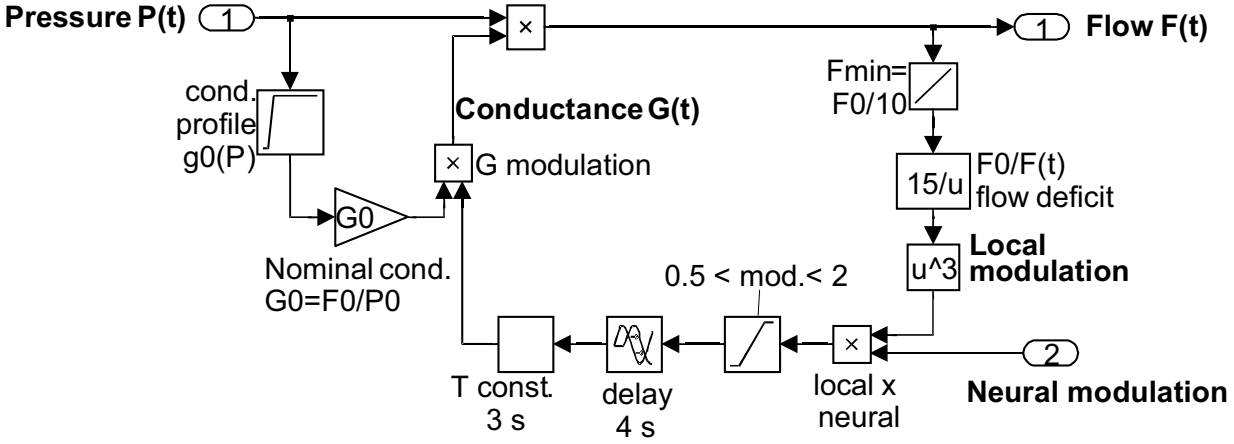

Fig.2 Model of peripheral vascular district (PVD). See text.

around the nominal driving pressure (P_0 = 60 mmHg) the PVD tends to compensate flow deviations from the nominal value F_0 = 15 ml/sec; 3) above the compensation range the regulation fails and flow imbalance takes place.

It is remarkable that a limit cycle with sustained oscillations of the flow control loop are present in the compensation range. The period of oscillations is proportionally related to the loop delay and negligibly affected by other parameters. In the proposed example it displays a value of 12 sec (0.8 Hz) in good accordance with the LF activity observed in peripheral vessels.

A PVD driven by a fixed flow equal to F_0 through a buffer compliance maintains an oscillating capability, provided that the compliance is sufficiently large. E.g. the 15 ml/sec PVD requires a compliance of 0.4 ml/mmHg to develop a limit cycle; the amplitude of conductance oscillations increases almost linearly up to 0.2 ml/(mmHg·sec) peak to peak (range 0.2÷0.4 around G_0=0.25) with a compliance of 0.7 ml/mmHg and next saturates. Oscillation period is invariant.

4. Two PVDs characteristics

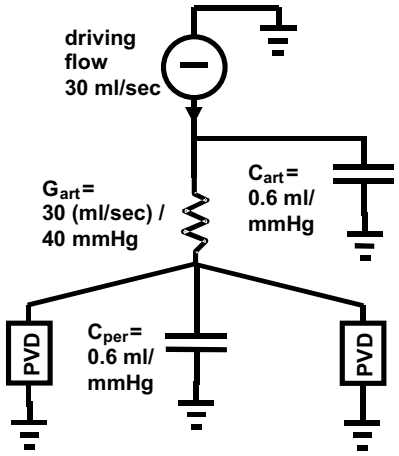

Fig. 3 - Model with two PVDs

The simplest study of PVD coupling is carried out on the scheme shown in Fig.3, where two PVDs are loading a single windkessel compliance. Resistances are adjusted in order to maintain a mean systemic AP of 100 mmHg over a peripheral pressure feeding the PVDs of 60 mmHg. The mean feeding flow is 30 ml/sec, that is matched to the nominal flows of the two PVDs. The compliance is adjusted in order to obtain a 120/80 mmHg pulsatile pressure when the system is driven by rectangular flow pulses of 200 msec over a 1 sec period. Due to windkessel buffering, negligible pulse is found in peripheral flows, conductances (see Fig.4, upper panel) and pressure (see Fig.4, lower panel, lower trace).

4.1. Unstable in-phase oscillations

The case of two identical PVDs is first considered (parameter values as in Fig.2). If both PVDs are initialized at exactly the same value (initial feedback modulation = 1) they keep behaving synchronously just as a single PVD of double size would do; the expected LF oscillations are observed both when the system is fed by a continuous and a pulsatile flow. The synchronous oscillation of flow uptake by the twin PVDs causes the compliance pressure (and consequently systemic AP) to display significant (10 mmHg peak to peak) oscillations.

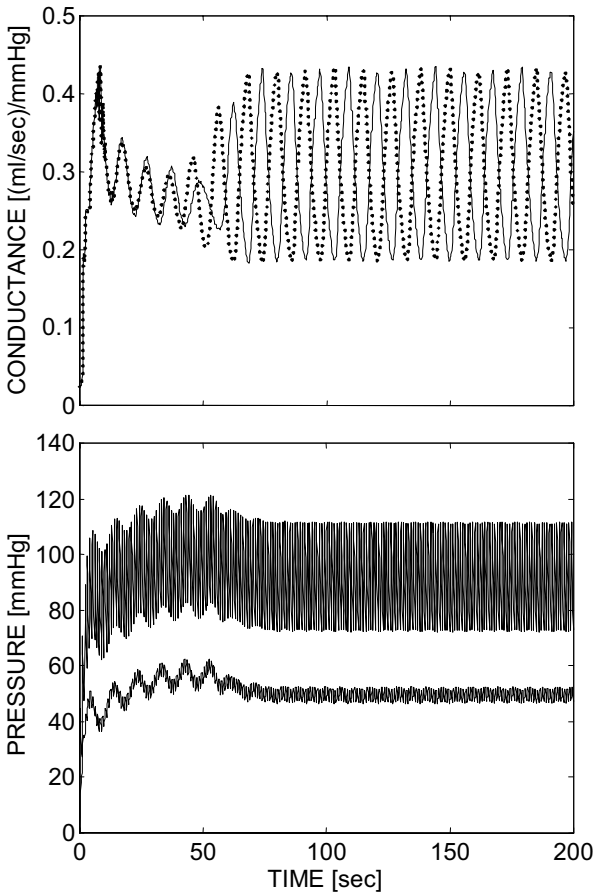

Fig.4 - Transition from the unstable in-phase peripheral oscillations to the stable phase opposition

This behavior would seem the most plausible; however, it is readily shown to represent an unstable solution of the model integration. In Fig.4, a simulation is shown in which the modulating feedbacks in the PVDs are initialized at 1.000 and 1.001 respectively. After the initial loading of the windkessel compliance the identical PVDs keep synchronization for the first LF cycles but then the unstable movement breaks out into a stable one.

4.2. Stable oscillations in phase opposition

The stable behavior was tested to be maintained indefinitely and to be insensitive to initial conditions. Its characteristics are: 1) larger peripheral LF oscillations clearly seen in the PVD flow, conductance and loading pressure; 2) phase opposition of the twin PVDs;

3) absence of LF oscillation in the systemic AP. The last feature is a direct consequence of phase opposition and of symmetry: only a residual half period ripple is present on the common compliance.

The stability of this behavior is supported by energetic analysis considering the mean power (flow times pressure drops) dissipated by the whole tree (and delivered by the flow generator) or in the single components. The in-phase solution required a mean power of 3045 mmHg·ml/sec, while, in the stable phase opposition movement, this figure decreased by a 9% to a value of 2783. The power consumption in the common resistance was almost equal in the two cases (1287 and 1284 respectively) while a 14% reduction was observed in both PVDs from 879 to 757 each.

4.3. Structural stability

Various conditions were tested to analyze the robustness of this feature. E.g. considering three identical PVDs, a stable LF oscillation was present with 120° phase differences among each PVD; therefore, also in this case maximum phase dispersion and maximum load equalization on the common compliance was achieved.

With two PVDs with progressively different natural frequencies the usual transition from 1:1 phase locking to quasiperiodicity was observed. PVD #1 was set as in Fig.2 (delay τ_1=4 sec), while the delay of PVD #2 was increased; so the system was described by ratio τ_2/τ_1. Phase locking was kept up to a 20% period difference (τ_2/τ_1=1.2): the slower PVD (#2) had a phase delay (in respect to phase opposition) that increased up to quadrature. Next the trajectories broke into quasi-periodicity describing first a narrow torus (τ_2/τ_1=1.3) which was then fully developed (τ_2/τ_1=1.6). Interestingly, the energy analysis revealed a smooth passage through these conditions with a slight increase of power consumption largely below the figure relevant to the unstable in-phase solution of two twin PVDs.

4.4. Neural in-phase synchronization

The 9% decrease in the overall power is sufficiently high to assure a robust stability to the phase opposition behavior but it is not large enough to prevent the system to switch on in-phase trajectories when the two (or more) PVDs are paced by a common neural modulation.

Simulations were carried out both introducing an external pacing at LF (central command) or a feedback driven by the systemic AP (baroreflex). In both cases even mild inputs or feedbacks led to in-phase peripheral oscillations and, therefore, disclosed the effects of the previously hidden peripheral vasomotor activity at systemic AP level.

5. Conclusions

Phase locking of similar oscillators is commonly conceived as in-phase; on the contrary the coupling of PVDs loading common compliance seems to privilege phase opposition or more generally maximum phase dispersion and appears to keep it robustly, until suitable neural drives are applied.

This behavior is in keeping with the experimental observation that small variability indices are observed at systemic level in correspondence to a very high activity in single districts [8].

The concept of neural control synchronizing the bulk of vasomotor activity can possibly disclose a new comprehension of AP waves and of their responsiveness to both autonomic and hemodynamic conditions.

References

[1] Malliani A, Pagani M, Lombardi F, Cerutti S. Cardiovascular neural regulation explored in the frequency domain. Circulation 1991; 84:482-92.

[2] Koepchen HP. History of studies and concepts of blood pressure waves. In: Miyakawa K, Polosa C, Koepchen HP, editors. Mechanisms of blood pressure waves. Berlin: Springer Verlag, 1984:3-23.

[3] Seydnejad SR, Kitney RI. Modeling of mayer waves generation mechanisms. IEEE Eng Med Biol Mag 2001; 20:92-100.

[4] De Boer RW, Karemaker JM, Strackee J. Hemodynamic fluctuations and baroreflex sensitivity in humans: a beat to beat model. Am J Physiol 1987; 253:680-9.

[5] Ursino M, Colantuoni A, Bertuglia S. Vasomotion and blood flow regulation in hamster skeletal muscle microcirculation: a theoretical and experimental study. Microvasc Res 1998; 56:233-52.

[6] Griffith TM, Edwards DH. Integration of non-linear cellular mechanisms regulating microvascular perfusion. Proc Instn Mech Engrs 1999; 213 Part H:369-83.

[7] Bernardi L, Hayoz D, Wenzel R, Passino C, Calciati A, Weber R, Noll G. Synchronous and baroreceptor-sensitive oscillations in skin microcirculation: evidence for central autonomic control. Am J Physiol 1997; 273:H1867-78.

[8] Porta A, Baselli G, Cerutti S, Lucini D, Della Vecchia M, Pagani M. Interaction between peripheral blood flow and low frequency components in cardiovascular variability signals. Computers in Cardiology 1999; 26:635-8.

Address for correspondence.

Giuseppe Baselli
Politecnico di Milano
Dip. di Bioingegneria
P.zza Leonardo da Vinci, 32
20133 Milano
Italy
E-mail address: baselli@biomed.polimi.it